Journal of Applied Mechanics and Technical Physics, Vol. 47, No. 1, pp. 91–98, 2006

PRESSURE RELAXATION IN A HOLE SURROUNDED BY POROUS AND PERMEABLE ROCK IN HOLE PRESSURE TESTS WITH GAS INJECTION

V. Sh. Shagapov,[1] I. G. Khusainov,[2] and R. M. Khafizov[2]

UDC 622.276.031

The pressure testing of a hole in porous and permeable rock by gas injection is considered. An integral equation for the hole pressure relaxation is obtained whose numerical and analytical solutions describe the dependence of the relaxation time of hole pressure on the reservoir properties of the surrounding porous rock as well as on the initial gas content and the initial pressure gradient in the hole.

Key words: *pressure relaxation, hole pressure testing, porous bed, fluid filtration, elastic capacity.*

Introduction. Pressure testing is a conventional method for determining the tightness of hydraulic systems. The main critical measure of the tightness of such systems is usually the satisfaction of certain permissible standards (depending on the particular technological conditions) for the pressure release rates in a system, which are determined by the fluid leakage rate [1, 2]. It seems that this method is also suitable for a more careful analysis of the state of wellbore zones in hydrodynamic tests of boreholes. After borehole pressure testing, the pressure relaxation rate in boreholes surrounded by porous rock depends on the reservoir properties of the surrounding porous rock. Hence, the pressure relaxation time can serve as a measure of, for example, the effective permeability coefficient of the rock around the borehole. Furthermore, adding a gas phase during pressure testing and thus increasing the elastic capacity of the medium in the borehole, it is possible to obtain characteristic relaxation time convenient for the practical implementation of this method.

1. Constitutive Equations. In the initial state ($t < 0$), let the fluid pressure over the entire porous bed around the hole be constant and equal to p_0' and the hole (a crack, cylindrical or spherical areas) be filled with a fluid. At the time $t = 0$, the pressure in the hole is increased instantaneously to a value p_0, for example, by injecting a certain amount of gas. Next, because of fluid filtration to the surrounding porous space, the hole pressure decreases to the value p_0'.

In describing these processes, we adopt the following assumptions: the hole pressure is uniform, there are no phase transitions and gas filtration through the walls of the hole, i.e., the mass of the gas in the hole remains constant throughout the process. This implies that in the practical implementation of the method considered, the gas phase should be in a special container which prevents it from entering the porous bed surrounding the hole (the injected gas volume should only work as a spring, displacing the fluid from the hole). For the one-dimensional plane problem, it is assumed that the hole (crack) walls are plane-parallel and the distance between them is far smaller than the linear dimensions of the walls. Fluid filtration occurs only through the front wall, and the remaining parts of the hole surface are impermeable. In the case of the radial problem, we assume that the length of the cylindrical hole is much greater than its radius and that the hole ends are impermeable.

Under the assumptions adopted above, the conservation equation for the mass of the fluid in the hole, the piezoconductivity equation, and the Darcy law for fluid filtration [3] are written as

[1]Institute of Mechanics, Ufa Scientific Center, Russian Academy of Sciences, Ufa 450000. [2]Sterlitamak State Pedagogical Institute, Sterlitamak 453103; tsur1@mail.ru, tsur1@rambler.ru, or tsur1@yandex.ru. Translated from Prikladnaya Mekhanika i Tekhnicheskaya Fizika, Vol. 47, No. 1, pp. 109–118, January–February, 2006. Original article submitted April 6, 2004; revision submitted March 3, 2005.

0021-8944/06/4701-0091

$$\frac{d\rho}{dt} = -\frac{n+1}{a}\,\rho_l u\Big|_{r=a}; \tag{1.1}$$

$$\frac{\partial p'}{\partial t} = \varkappa\,\frac{1}{r^n}\,\frac{\partial}{\partial r}\Big(r^n\,\frac{\partial p'}{\partial r}\Big), \qquad u' = -\frac{k}{\mu_l}\,\frac{\partial p'}{\partial r}, \qquad a < r < \infty. \tag{1.2}$$

Here a is the radius of the hole, μ_l and $\rho = \rho_l(1-\alpha_g)$ are the viscosity and density of the fluid, respectively, α_g is the volumetric fraction of the gas in the hole, $\varkappa = k\rho_{l0}C_l^2/(m\mu_l)$ is the piezoconductivity, m and k are the porosity and permeability, C_l is the sound velocity in the fluid, p' and u' are the pressure and filtration rate around the hole, u is the rate of fluid filtration through the hole walls, the superscripts $n = 0$, 1, 2 correspond to the one-dimensional plane, radial, and spherical problems, respectively. The compressibility of the fluid in the hole and in the porous bed is taken into account in the acoustic approximation, and the gas behavior follows a polytropic law, then,

$$p = p_0 + C_l^2(\rho_l - \rho_{l0}), \qquad \alpha_g = \alpha_{g0}(p_0/p)^{1/\gamma}, \tag{1.3}$$

where γ is the polytropic exponent and p_0 is the initial hole pressure. Here and below, the superscript 0 corresponds to the initial values.

The initial and boundary conditions for Eq. (1.2) are written as

$$p' = p'_0 \quad (t = 0, \quad r > a), \qquad p' = p(t), \quad u' = u \quad (t > 0, \quad r = a). \tag{1.4}$$

During pressure testing and in the subsequent period of pressure relaxation, the fluid density varies insignificantly ($\rho_l - \rho_{l0} \ll \rho_l$); therefore, on the right of Eq. (1.1), we ignore this variation, assuming that $\rho_l = \rho_{l0}$. Next, integrating Eq. (1.1) over time from 0 to t, we have

$$\rho_l(1-\alpha_g) - \rho_{l0}(1-\alpha_{g0}) = -\frac{n+1}{a}\,\rho_{l0}\int\limits_0^t u\Big|_{r=a}\,dt. \tag{1.5}$$

Substituting the parameters ρ_l and α_g from (1.3) into Eq. (1.5), we obtain the following dependence of the hole pressure on the rate of fluid filtration through the hole walls:

$$\alpha_{g0}\Big(\Big(\frac{p_0}{p}\Big)^{1/\gamma} - 1\Big) - \frac{p-p_0}{\rho_{l0}C_l^2}\Big(1 - \alpha_{g0}\Big(\frac{p_0}{p}\Big)^{1/\gamma}\Big) = -\frac{n+1}{a}\,\frac{k}{\mu_l}\int\limits_0^t \frac{\partial p'}{\partial r}\Big|_{r=a}\,dt. \tag{1.6}$$

In the case of low pressure testing ($\Delta p_0 = p_0 - p'_0 \ll p_0$), linearization reduces Eq. (1.6) to the form

$$\Delta P - 1 = \frac{(n+1)k\gamma p'_0}{\mu_l a(\alpha_{g0} + \gamma\sigma(1-\alpha_{g0}))}\int\limits_0^t \frac{\partial \Delta P'}{\partial r}\Big|_{r=a}\,dt$$

$$\Big(\Delta P = \frac{\Delta p}{\Delta p_0}, \quad \Delta P' = \frac{\Delta p'}{\Delta p_0}, \quad \Delta p = p - p'_0, \quad \Delta p_0 = p_0 - p'_0, \quad \Delta p' = p' - p'_0, \quad \sigma = \frac{p'_0}{\rho_{l0}C_l^2}\Big).$$

2. One-Dimensional Plane Problem ($n = 0$, $r = x$). Using the Duhamel principle [4–7] for Eq. (1.2) with the variable boundary conditions (1.4), we obtain the following solution for the pressure profile in a porous bed around the hole:

$$p' - p'_0 = \int\limits_0^t \frac{\partial U(x, t-t')}{\partial t}\,(p(t') - p'_0)\,dt', \tag{2.1}$$

$$U(x,t) = \Phi\Big(\frac{x-a}{2\sqrt{\varkappa t}}\Big), \qquad \Phi(\xi) = 1 - \frac{2}{\sqrt{\pi}}\int\limits_0^\xi \exp(-\lambda^2)\,d\lambda \qquad (x > a,\ t > 0).$$

Here the function $U(x,t)$ is a solution of the piezoconductivity equation (1.2) subject to constant boundary conditions and zero initial conditions.

Transforming Eq. (1.6) with the use of solution (2.1) and the Darcy law, we obtain the following integral equation for the hole pressure relaxation:

$$\alpha_{g0}\Big(\Big(\frac{p_0}{p}\Big)^{1/\gamma}-1\Big)-\frac{p-p_0}{\rho_{l0}C_l^2}\Big(1-\alpha_{g0}\Big(\frac{p_0}{p}\Big)^{1/\gamma}\Big)=\frac{k}{a\mu_l\sqrt{\pi\varkappa}}\int\limits_0^t\frac{p(t')-p_0'}{\sqrt{t-t'}}\,dt'. \tag{2.2}$$

In the case of low pressure testing, this implies that

$$1-\Delta P=\int\limits_0^t\frac{\Delta P(t')}{\sqrt{\pi(t-t')\tilde t}}\,dt',\quad \tilde t=\beta^2 t_a,\quad t_a=\frac{a^2}{\varkappa},\quad \beta=\frac{\alpha_{g0}+\gamma\sigma(1-\alpha_{g0})}{\gamma m\sigma}. \tag{2.3}$$

Here t_a is the characteristic time in which the pressure perturbation in the neighborhood of the hole propagates over the porous bed for a distance of about half-width of the hole a (the radius in the radial and spherical cases).

Equation (2.3) has an analytical solution. Indeed, applying a Laplace transform, it is easy to obtain the image

$$\Delta\hat P=\frac{1}{q+\sqrt{q/\tilde t}},\qquad \Delta\hat P=\int\limits_0^\infty\exp(-qt)\Delta P(t)\,dt.$$

This image is tabulated [8], and for the solution of the integral equation (2.3), we can write

$$\Delta P=\exp(\tau)\Phi(\sqrt{\tau}\,)\qquad(\tau=t/\tilde t). \tag{2.4}$$

This solution coincides with the solution of the problem of cooling of an ideal heat conductor in a different medium [9].

The pressure relaxation dynamics in the initial ($\tau\ll1$) and final ($\tau\gg1$) stages can be described by the simpler relations

$$\Delta P=1-\frac{2}{\sqrt{\pi}}\sqrt{\tau}+\tau+O(\tau),\qquad \Delta P=\frac{1}{\sqrt{\pi\tau}}\Big(1-\frac{1}{\tau}+O\Big(\frac{1}{\tau}\Big)\Big). \tag{2.5}$$

Numerical analysis shows that the first formula of (2.5) is adequate for describing the hole pressure relaxation in the initial stage up to $\tau\approx10^{-1}$, and the second formula for $\tau\geqslant10$. Using the second formula of (2.5), it is possible to obtain a simple estimate for the time of full pressure relaxation in the hole t_r. According to the solutions obtained, the pressure relaxation, generally speaking, occurs in infinite time ($t_r\to\infty$). Therefore, here and below, as the characteristic time of complete pressure relaxation, we use the time in which the dimensionless pressure gradient ΔP in the hole decreases to $\Delta P=10^{-2}$. Then, based on (2.5), the dimensionless relaxation time is $\tau_r\approx3200$. From this value of τ_r, it is easy to obtain the dependence of the dimensional relaxation time t_r on the parameters of the system:

$$t_r=\tau_r\beta^2t_a=\tau_r\,\frac{m\mu_la^2}{k\rho_{l0}C_l^2}\Big[\frac{\alpha_{g0}+\gamma\sigma(1-\alpha_{g0})}{\gamma m\sigma}\Big]^2. \tag{2.6}$$

We note that according to (2.6), the relaxation time in all cases is inversely proportional to the permeability coefficient.

We give some numerical estimates for the case of a hole containing the water–air system ($\rho_{l0}=10^3$ kg/m^3, $C_l=1.5\cdot10^3$ m/sec, and $\gamma\approx1$–1.4) at $p_0'=1$ MPa. The dimensionless parameter $\sigma\approx0.4\cdot10^{-3}$. Therefore, with the addition of a small gas volume (in this case, for $\alpha_{g0}\geqslant10^{-3}$) the elastic capacity of the hole is completely determined by the elastic capacity of the gas phase. For the low volumetric gas contents satisfying the condition $\alpha_{g0}\ll\sigma$, the presence of the gas has no effect on the hole pressure relaxation. In this case, from (2.6) we have

$$t_r=\tau_r\mu_la^2/(mk\rho_{l0}C_l^2).$$

For the case of high pressure testing ($\Delta p_0\geqslant p_0'$), calculations were performed using the integral equation (2.2). The calculation algorithm was tested by the analytical solution (2.4). In Fig. 1, the solid curves show results of numerical calculations for the pressure relaxation process at different initial pressures in the hole. The parameters of the hole, porous bed, fluid, and gas have the following values: $a=10^{-2}$ m, $m=0.1$, $k=10^{-12}$ m^2, $p_0'=1$ MPa, $\rho_{l0}=10^3$ kg/m^3, $C_l=1.5\cdot10^3$ m/sec, $\mu_l=0.001$ Pa$\cdot$,sec, and $\gamma=1.4$. Unless otherwise specified, the same values

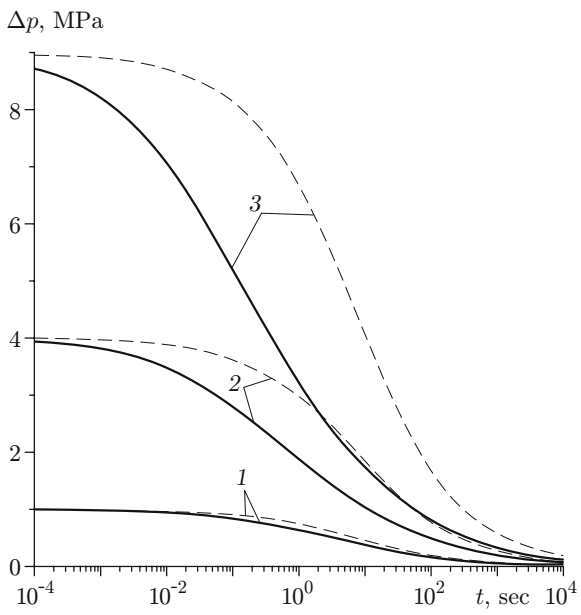

Fig. 1

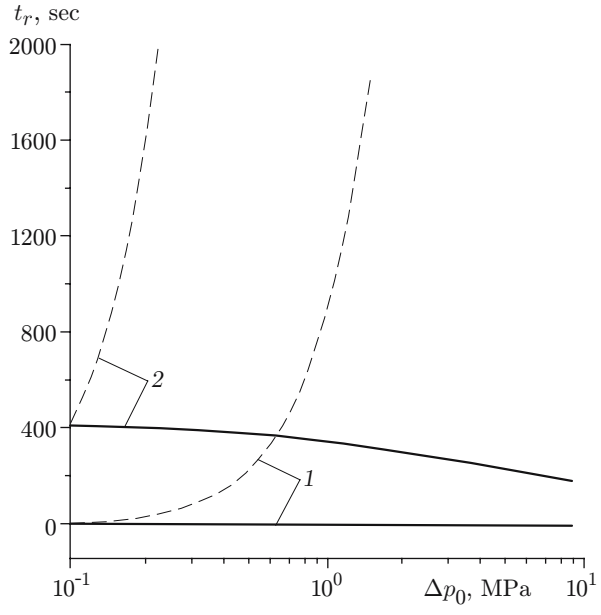

Fig. 2

Fig. 1. Pressure evolution in a hole with plane–parallel walls: the solid curves refer to the numerical solutions of Eq. (2.2) and the dashed curves refer to the anaytical solution (2.4); curves 1, 2, and 3 refer to $p_0 = 2$, 5, and 10 MPa, respectively.

Fig. 2. Relaxation time versus initial pressure gradient for a hole with plane–parallel walls for $\alpha_{g0} = 10^{-3}$ (1) and 10^{-2} (2).

for the parameters of the hole–porous bed system are used in the subsequent numerical examples. In all versions, the initial volumetric gas content is $\alpha_{g0} = 10^{-1}$. The dashed curves in Fig. 1 correspond to the analytical solution (2.4). It is evident that in the case of low pressure testing ($\Delta p_0 = 1$ MPa; curves 1), the analytical solution (2.4) is in good agreement with the numerical solution of (2.2). However, as Δp_0 increases, the difference between these solutions becomes larger. In particular, for $\Delta p_0 = 9$ MPa, as follows from the behavior of curves 3, the solution of the linearized equation considerably overestimates the relaxation time in the final stage of the relaxation process. Here we note that in the case of pressure testing without gas injection ($\alpha_{g0} = 0$), the relaxation process for all initial pressure gradients Δp_0 is described by the analytical solution (2.4). Thus, pressure testing with gas injection leads to a considerable increase in the relaxation time due to both a direct increase in the elastic capacity of the hole with gas injection and the nonlinear pressure dependence of the average density of the gas–fluid system in the hole.

Figure 2 shows curves of the relaxation time versus the initial pressure gradient Δp_0 ($\Delta p_0 = p_0 - p_0'$) for various initial volumetric gas contents. It is evident that the larger α_{g0}, the stronger the dependence of the relaxation time t_r on the pressure gradient Δp_0. Here and below, in the construction of the solid curves, the relaxation time t_r corresponds to the period in which the value of ΔP decreases to 10^{-2}; for the dashed curves, we use a physical criterion according to which the relaxation time is the period in which the gradient Δp decreases to $\Delta p_* = 1$ kPa irrespective of the initial pressure gradient Δp_0. Thus, it follows from Fig. 2 that by these two criteria, the behavior of the dependence of the relaxation time on the initial pressure gradient varies not only quantitatively but also qualitatively. By the first criterion, this dependence decreases monotonically, whereas by the second criterion, it increases. This difference in the behavior is due to a manifestation of the nonlinear nature of the relaxation process with increasing initial pressure gradient Δp_0.

3. Radial Problem ($n = 1$)**.** For the radial problem, the solution of Eq. (1.2) subject to conditions (1.4) can also be written similarly to expressions (2.1). In this case, the function U has the form

$$U(r,t) = \frac{1}{2\pi i} \int\limits_{\sigma-i\infty}^{\sigma+i\infty} \frac{\exp(\lambda t) K_0(\sqrt{\lambda/\varkappa}\, r)}{K_0(\sqrt{\lambda/\varkappa}\, a)} \frac{d\lambda}{\lambda}, \tag{3.1}$$

where $K_0(w)$ is a Macdonald function of zero order. As is known [9], function (3.1), in turn, can be written as

$$U(r,t) = 1 + \frac{2}{\pi}\int\limits_0^\infty \exp\Big(-\frac{z^2 t}{t_a}\Big)\,\frac{J_0(zr/a)Y_0(z) - J_0(z)Y_0(zr/a)}{J_0^2(z) + Y_0^2(z)}\,\frac{dz}{z},$$

where $J_0(v)$ and $Y_0(v)$ are Bessel and Neumann functions of zero order. Then, the equation describing the pressure evolution in a cylindrical hole becomes

$$\alpha_{g0}\Big(\Big(\frac{p_0}{p}\Big)^{1/\gamma} - 1\Big) - \frac{p - p_0}{\rho_{l0} C_l^2}\Big(1 - \alpha_{g0}\Big(\frac{p_0}{p}\Big)^{1/\gamma}\Big) = \frac{k}{a^2\mu_l}\int\limits_0^t \varphi\Big(\frac{t-t'}{t_a}\Big)(p(t') - p_0')\,dt',$$

$$\varphi(S) = \frac{8}{\pi^2}\int\limits_0^\infty \frac{\exp(-Sz^2)}{J_0^2(z) + Y_0^2(z)}\,\frac{dz}{z}. \tag{3.2}$$

In the case of low pressure testing ($\Delta p_0 = p_0 - p_0' \ll p_0$) from Eq. (3.2) we have

$$1 - \Delta P = \frac{1}{\beta t_a}\int\limits_0^t \varphi\Big(\frac{t-t'}{t_a}\Big)\,\Delta P(t')\,dt'. \tag{3.3}$$

Applying a Laplace transform to Eq. (3.3), we obtain

$$\Delta P = \frac{1}{\pi}\int\limits_0^\infty \frac{\phi\sin\xi t - \psi\cos\xi t}{\xi(\phi^2 + \psi^2)}\,d\xi,$$

where

$$\phi = 1 + \frac{8}{\pi^2\beta}\int\limits_0^\infty \frac{v\,dv}{(\xi^2 t_a^2 + v^4)(J_0^2(v) + Y_0^2(v))}, \qquad \psi = \frac{8\xi t_a}{\pi^2\beta}\int\limits_0^\infty \frac{dv}{v(\xi^2 t_a^2 + v^4)(J_0^2(v) + Y_0^2(v))}.$$

The solution of this equation is cumbersome but does not involve serious difficulties.

The core of the integral equation (3.2) for small values of the argument can be expanded as follows [9]:

$$\varphi(S) = \frac{2}{\sqrt{\pi S}} + 1 - \frac{1}{2}\sqrt{\frac{S}{\pi}} + \frac{S}{4} + \dots\ .$$

For large values of the argument, the following formula is valid:

$$\varphi(S) = 4/\ln(4S/\Gamma), \qquad \Gamma = \exp(2C), \qquad C = 0.577\,22\dots\ .$$

Here C is the Euler constant.

According to [10], for the time interval $0 < t \leqslant 10t_a$, we can use the following approximation for the core:

$$\varphi(S) = 2/\sqrt{\pi S} + 1.$$

In this case, the integral equation (3.3) becomes

$$1 - \Delta P = \frac{1}{\beta t_a}\int\limits_0^t \Big(1 + \frac{2}{\sqrt{\pi(t-t')/t_a}}\Big)\,\Delta P(t')\,dt'. \tag{3.4}$$

The solution of Eq. (3.4) can be written as

$$\Delta P = \mathrm{Re}\,\{[\beta_+ \exp(\beta_+^2\tau)\Phi(\beta_+\sqrt{\tau}) - \beta_- \exp(\beta_-^2\tau)\Phi(\beta_-\sqrt{\tau})]/(\beta_+ - \beta_-)\},$$
$$\beta_- = 1 - \sqrt{1-\beta}, \qquad \beta_+ = 1 + \sqrt{1-\beta}. \tag{3.5}$$

Solution (3.5) describes the dynamics of the initial stage of pressure relaxation in the hole. If the relaxation time t_r satisfies the condition $t_r \leqslant 10t_a$, this solution can be used for the entire period of relaxation. In this case, for the final relaxation stage, $\tau_r \approx 1/\beta$ or $t_r \approx \beta t_a$.

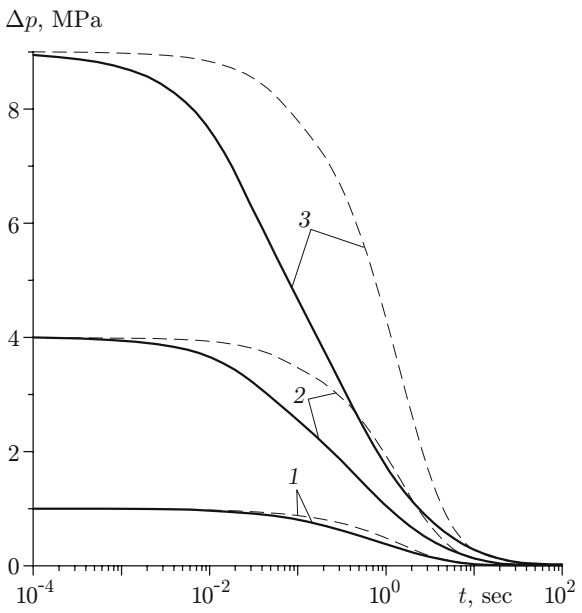

Fig. 3

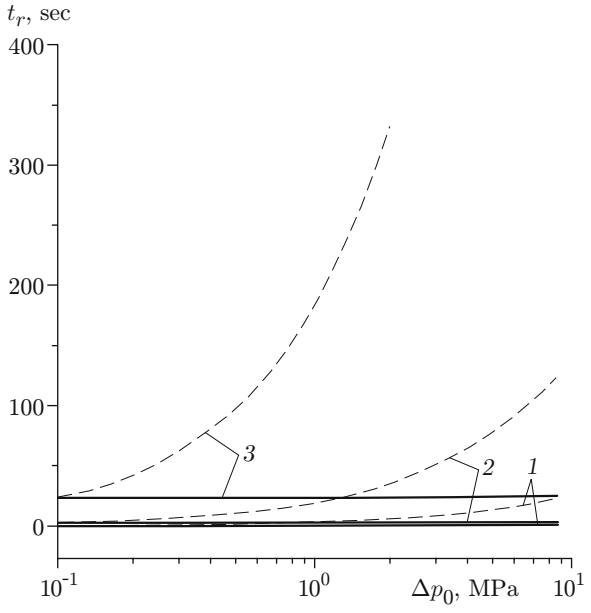

Fig. 4

Fig. 3. Effect of the initial pressure in a cylindrical hole on the pressure relaxation dynamics: the solid curves refer to the numerical solutions of Eq. (3.2); the dashed curves refer to the numerical solutions (3.3); curves 1, 2, and 3 refer to $p_0 = 2$, 5, and and 10 MPa.

Fig. 4. Relaxation time in a cylindrical hole versus initial pressure gradient for $\alpha_{g0} = 10^{-3}$ (curves 1), 10^{-2} (curves 2), and 10^{-1} (curves 3).

Thus, solution (3.5) can be used during the entire period of relaxation provided that $\beta \leqslant 10$. From an analysis of formula (2.3) for β, it follows that the condition $\beta \leqslant 10$ is reached in the case of pressure testing without gas injection. For $\alpha_{g0} = 0$, we have $\beta = 1/m$; therefore, for the porous bed, we have $m \geqslant 10^{-1}$.

For the final stage of the pressure relaxation, a somewhat different approximate analytical solution can be constructed. We assume that in this stage, beginning with a certain time t_* ($t > t_*$), the current pressure gradient in the hole and the rate of liquid flow through the hole walls satisfy the expression

$$u\Big|_{r=a} = \frac{2(p - p_0')k}{\mu_l a \ln\left(4t/(\Gamma t_a)\right)}, \tag{3.6}$$

which follows from the well-known self-similar solution [11] for $t \gg t_a$. Then, substituting (3.6) into (1.1) for $n = 1$, we obtain a solution in the form of the following quadrature for the final stage of pressure relaxation:

$$\int\limits_{p_*}^{p} \frac{(1-\alpha_g)/C_l^2 + \rho_l \alpha_g/(\gamma p)}{p - p_0'}\, dp = -\frac{4k\rho_{l0}}{a^2 \mu_l} \int\limits_{t_*}^{t} \frac{dt'}{\ln\left(4t'/(\Gamma t_a)\right)}. \tag{3.7}$$

Here p_* is the hole pressure at the time $t = t_*$, α_g and ρ_l are the pressure functions from (1.3). In the case of low pressure testing, from (3.7), we have

$$\Delta p = \Delta p_* \exp\Big(-\frac{4}{\beta t_a} \int\limits_{t_*}^{t} \frac{dt'}{\ln\left(4t'/(\Gamma t_a)\right)}\Big), \qquad \Delta p_* = p_* - p_0'.$$

Figure 3 shows the pressure relaxation dynamics in a cylindrical hole of radius $a = 10^{-1}$ m for $\alpha_{g0} = 10^{-1}$ and various initial pressures. It is evident that in the case of a cylindrical hole, the solution of the linearized equations (3.3) underestimates the relaxation time compared to the numerical solution of the general nonlinear equation (3.2) and this difference becomes larger with increasing p_0.

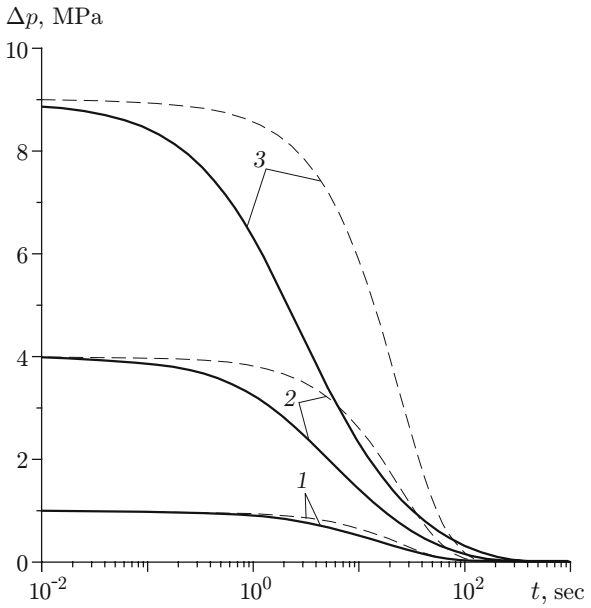

Fig. 5. Pressure relaxation in a spherical hole at $p_0 = 2$ (1), 5 (2) and 10 MPa (3): the solid curves refer to the numerical solution of (4.2) and the dashed curves refer to the analytical solution (3.5) with the dimensionless parameters (4.4).

Figure 4 gives curves of the relaxation time versus initial pressure gradient for various initial volumetric gas contents. It is evident that in the case of a cylindrical hole, the relaxation time also depends strongly on the initial gas content. Unlike in the plane case, this dependence increases monotonically for both the first and second criteria.

4. Spherical Problem ($n = 2$). As in the previous two cases, the solution for a spherical hole can be written as (2.1); in this case,

$$U(r,t) = \frac{a}{r}\,\Phi\Big(\frac{r-a}{2\sqrt{\varkappa t}}\Big). \tag{4.1}$$

Taking into account (4.1), we obtain the following integral equation for the pressure relaxation in a spherical hole:

$$\alpha_{g0}\Big(\Big(\frac{p_0}{p}\Big)^{1/\gamma} - 1\Big) - \frac{p-p_0}{\rho_{l0}C_l^2}\Big(1 - \alpha_{g0}\Big(\frac{p_0}{p}\Big)^{1/\gamma}\Big) = \frac{3k}{a^2\mu_l}\int\limits_0^t \Big(1 + \frac{1}{\sqrt{\pi(t-t')/t_a}}\Big)(p(t') - p_0')\,dt'. \tag{4.2}$$

In the case of low pressure testing ($\Delta p_0 = p_0 - p_0' \ll p_0$), we have

$$1 - \Delta P = \frac{3}{\beta t_a}\int\limits_0^t \Big(1 + \frac{1}{\sqrt{\pi(t-t')/t_a}}\Big)\Delta P(t')\,dt'. \tag{4.3}$$

Ignoring unity compared to the second term of the core of the integral equation (4.3), we obtain an equation similar to (2.3) for the initial stage of pressure relaxation ($t \ll t_a$). In this case, the coefficient on the right side is equal to three. Consequently, in a spherical hole, the pressure relaxation rate in the initial stage is higher than that in the previous two cases.

Equation (4.3) has an exact analytical solution which is similar in form to (3.5); in this case, for the dimensionless parameters, we have

$$\beta_- = (3/2)(1 - \sqrt{1 - 4\beta/3}), \qquad \beta_+ = (3/2)(1 + \sqrt{1 - 4\beta/3}). \tag{4.4}$$

Figure 5 gives curves which illustrate the pressure relaxation dynamics in a spherical hole of radius $a = 1$ m for an initial volumetric gas content of $\alpha_{g0} = 10^{-1}$. We note that the data given in the figure agree qualitatively with the results for the case of a cylindrical hole.

Conclusions. Hole pressure testing by injection of a certain amount of gas increases the elastic capacity of the hole, which, in turn, leads to an increase in the characteristic pressure relaxation time. The nonlinear nature of the relaxation process is manifested as the initial pressure gradient Δp_0 is increased. Therefore, in hydrodynamic pressure tests of open boreholes (aimed for example at determining the permeability coefficient), gas injection and variation of the initial pressure gradient Δp_0 enable one to control the characteristic pressure relaxation time.

This work was supported by the Russian foundation for Basic Research (Grant No. 05-01-97919).

REFERENCES

1. K. V. Iogansen, *Handbook of the Drill Man* [in Russian], Nedra, Moscow (1990).
2. M. L. Karnaukhov and N. F. Ryazantsev, *Handbook on Borehole Testing* [in Russian], Nedra, Moscow (1984).
3. K. S. Basniev, I. N. Kochina, and V. M. Maksimov, *Underground Hydrodynamics* [in Russian], Nedra, Moscow (1993).
4. M. Musket, *The Flow of Homogeneous Fluids through Porous Media*, McGraw-Hill, New York (1937).
5. R. Collins, *Flow of Fluids through Porous Materials*, Reinhold, New York (1961).
6. S. N. Buzinov and I. D. Umrikhin, *Hydrodynamic Method of Testings of Wells and Seams* [in Russian], Nedra, Moscow (1973).
7. A. M. Pirverdin, *Physics and Hydraulics of an Oil Reservoir* [in Russian], Nedra, Moscow (1982).
8. V. A. Ditkin and A. P. Prudnikov, *Handbook on Operational Calculus* [in Russian], Vysshaya Shkola, Moscow (1965).
9. H. S. Carslaw and J. C. Jaeger, *Conduction of Heat in Solids*, Oxford Univ. Press, London (1959).
10. V. Sh. Shagapov, G. Ya. Khusainova, I. G. Khusainov, and R. M. Khafizov, "Pressure relaxation in a hole surrounded by porous and permeable rock," *Combust., Expl., Shock Waves*, **38**, No. 3, 346–351 (2002).
11. G. I. Barenblatt, V. M. Entov, and V. M. Ryzhik, *Motion of Fluids and Gases in Natural Reservoirs* [in Russian], Nedra, Moscow (1984).